Vol 17 No 2, February 2008
1674-1056/2008/17(02)/0373-07
Chinese Physics B
© 2008 Chin. Phys. Soc.
and IOP Publishing Ltd

A dynamic epidemic control model on uncorrelated complex networks*

Pei Wei-Dong(裴伟东)[a)b)†], Chen Zeng-Qiang(陈增强)[a)], and Yuan Zhu-Zhi(袁著祉)[a)]

[a)] *Department of Automation, Nankai University, Tianjin* 300071, *China*

[b)] *College of Computer and Information Engineering, Tianjin Normal University, Tianjin* 300387, *China*

(Received 22 May 2007; revised manuscript received 15 August 2007)

In this paper, a dynamic epidemic control model on the uncorrelated complex networks is proposed. By means of theoretical analysis, we found that the new model has a similar epidemic threshold as that of the susceptible-infected-recovered (SIR) model on the above networks, but it can reduce the prevalence of the infected individuals remarkably. This result may help us understand epidemic spreading phenomena on real networks and design appropriate strategies to control infections.

Keywords: complex networks, dynamic quarantining mechanism, QSIR model, epidemic threshold
PACC: 0250, 0565, 0520, 8000

1. Introduction

Controlling the spreading of diseases on real world networks is one of the issues most concerned today. Many strategies on how to control the spreading of diseases have been proposed.[1−19] These strategies can be classified into two main groups: static and dynamic. The static immunization strategies proposed by Hu and Tang,[3] Barthelemy *et al*,[4] static content-filtering and address-blacklisting proposed by Moore *et al*,[5] static traffic-blocking proposed by Williamson *et al*[6] are among the first group. The biggest weakness of the static controlling strategies is the assumption that the strategies can only change the configuration of the network at the beginning of the epidemic spreading process but cannot do so during the spreading process, which is unreal in controlling diseases. Dynamic control strategies studied by Wong *et al*,[11] Boguñá *et al*[12] and Zou *et al*[13] have brought us some encouraging results for slowing down the spreading of diseases. However, since the dynamic control strategies are time-dependent, i.e. the strategies change their tactics according to the situation of the disease propagation during the whole epidemic process, the configuration of the network changes, depending not only on the propagation of the disease but also on the controlling strategies. This brought us some difficulties to analyse the epidemic process theoretically.

The purpose of this paper is to propose a new dynamical epidemic control model and provide theoretical analysis and simulations on the uncorrelated complex networks. In real networks such as social and computer networks, statistical observations show that the disease and virus incidents in the wild is saturated to a very low level of persistence. This fact is in striking contradiction with the theoretical predictions by the classical epidemic models such as the susceptible-infected (SI), the susceptible-infected-susceptible (SIS) and the susceptible-infected-recovered (SIR) models.[14−19] This is why we want to propose a new model in this paper.

Recently, Liu *et al*[15] proposed a feedback mechanism to study the spreading of epidemics. They modified the SIS model by adding a feedback mechanism: each individual can perceive the present density of infected individuals of the network, and therefore the edges of each node will be 'cut off' temporarily with a probability related to this density. Their simulation results show that by introducing the feedback mechanism, the density of infected individuals can be re-

*Project supported by the National Natural Science Foundation of China (Grant No. 60774088), the Program for New Century Excellent Talents of Higher Education of China (Grant No NCET 2005-290), the Special Research Fund for the Doctoral Program of Higher Education of China (Grant No 20050055013).
†Corresponding author. E-mail: paulpeiart@mail.nankai.edu.cn

duced remarkably. However, their work only focused on the SIS model and their result could only be applied to the exponential networks.

Motivated by their idea, we propose a new dynamic control model on the uncorrelated scale-free networks, which is more realistic than the exponential networks. Besides, our model is based on the SIR model, not the SIS model. In the new model, each individual in the network has one of four possible states: quarantined, susceptible, infected and recovered. For convenience, we shall call it the QSIR model according to its four states. The new added state (quarantined state) to the SIR model is based on the present probability that any given edge points to an infected node on the uncorrelated complex networks. Obviously, the larger the probability is, and the more the connections an individual owns, the more likely the individual will be quarantined. We have given a rigorous theoretical analysis and extensive simulations on the new model. The rest of the paper is organized as follows. In Section 2, we briefly review the classical SIR model and its main results. In Section 3, we give a rigorous theoretical analysis to the spreading threshold of the QSIR model. Section 4 gives extensive simulations by using the QSIR model on several different Barabási–Albert (BA) networks to compare its results with those of the SIR model. Finally, we give a conclusion in Section 5.

2. Review of SIR model

In the classical SIR model, each of the N nodes of the network can be in one of three possible states: susceptible, infected and recovered. At one time step, if a susceptible node has an infected neighbour, it will become infected with a probability λ (λ is also called the spreading rate of the infection). At the same time, each infected node will become recovered state with a probability μ (without loss of generality, the value of μ can be set at 1). If we use S, I and R to denote the susceptible, infected and recovered state respectively, then the epidemic process of the SIR model can be described by the following chart.

$$\mathrm{S} \xrightarrow{\lambda} \mathrm{I} \xrightarrow{1} \mathrm{R}$$

Suppose $s_k(t)$, $\rho_k(t)$ and $r_k(t)$ are the densities of the susceptible, infected and recovered nodes with degree k at time step t of the epidemic process respectively, then they satisfy the normalization condition

$$s_k(t) + \rho_k(t) + r_k(t) = 1. \tag{1}$$

On a complex network with a general degree distribution $p(k)$ and a finite average degree $\langle k\rangle = \sum_k kp(k)$ (k is the degree of a node and $p(k)$ the probability of nodes with degree k), these densities satisfy the following set of coupled differential equations (see Ref.[9]):

$$\frac{\mathrm{d}s_k(t)}{\mathrm{d}t} = -\lambda k s_k(t)\theta(t), \tag{2}$$

$$\frac{\mathrm{d}\rho_k(t)}{\mathrm{d}t} = -\rho_k(t) + \lambda k s_k(t)\theta(t), \tag{3}$$

$$\frac{\mathrm{d}r_k(t)}{\mathrm{d}t} = \rho_k(t), \tag{4}$$

where $\theta(t)$ is the probability that any given edge points to an infected node on the uncorrelated complex networks, which satisfies

$$\theta(t) = \frac{\sum_k kp(k)\rho_k(t)}{\sum_s sp(s)} = \frac{\sum_k kp(k)\rho_k(t)}{\langle k\rangle}. \tag{5}$$

With the initial conditions $s_k(0) \approx 1$, $\rho_k(0) \approx 0$, $r_k(0) = 0$ and the final epidemic condition $\rho_k(\infty) = 0$, the above equations will give the following result,

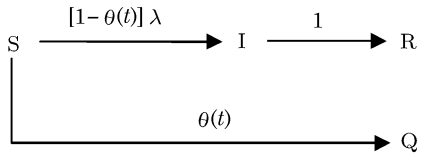
$$\lambda_{\mathrm{c}} = \frac{\langle k\rangle}{\langle k^2\rangle}, \tag{6}$$

where $\langle k^2\rangle = \sum_k k^2 p(k)$ and λ_{c} is the epidemic threshold, below which the epidemic prevalence is null, and above which it attains a finite value. For regular and exponential networks (in which $\langle k^2\rangle < \infty$), the threshold has a finite value. On the other hand, complex networks with strongly fluctuating connectivity distribution such as scale-free networks, show a vanishing epidemic threshold when increasing network sizes; i.e. $\langle k^2\rangle \to \infty$ when $N \to \infty$, or $\lambda_{\mathrm{c}} \to 0$ when $N \to \infty$, which means that the epidemic threshold λ_{c} is very small for large complex networks.

3. QSIR model and its theoretical analysis

In the quarantined-SIR (QSIR) model, we presume that each of the N nodes of the network can be in one of the four possible states: quarantined, susceptible, infected and recovered. At any time step t, a susceptible node will become quarantined with a probability $\theta(t)$, which is defined by Eq.(5). At the same time, if a susceptible node does have an infected

neighbour, it will become infected with a probability $\lambda[1-\theta(t)]$. Meanwhile, each infected node will become recovered state with a probability 1. If we use Q, S, I and R to denote the quarantined, susceptible, infected and recovered state respectively, then the epidemic process of the QSIR model can be described by the following chart:



Suppose that $s_k(t)$, $\rho_k(t)$, $r_k(t)$ and $q_k(t)$ are the densities of the susceptible, infected, recovered and quarantined nodes with degree k at time step t of the epidemic process respectively, then they satisfy the normalization condition

$$s_k(t)+\rho_k(t)+r_k(t)+q_k(t)=1. \tag{7}$$

With the analysis similar to that in Ref.[9], we can obtain that on the complex network with a general degree distribution $p(k)$ and a finite average degree $\langle k\rangle=\sum_k kp(k)$, these densities satisfy the following set of coupled differential equations

$$\frac{\mathrm{d}s_k(t)}{\mathrm{d}t}=-[1-\theta(t)]\lambda k s_k(t)\theta(t)-s_k(t)\theta(t), \tag{8}$$

$$\frac{\mathrm{d}\rho_k(t)}{\mathrm{d}t}=-\rho_k(t)+[1-\theta(t)]\lambda k s_k(t)\theta(t), \tag{9}$$

$$\frac{\mathrm{d}r_k(t)}{\mathrm{d}t}=\rho_k(t), \tag{10}$$

$$\frac{\mathrm{d}q_k(t)}{\mathrm{d}t}=s_k(t)\theta(t). \tag{11}$$

It is easy to verify that the above equations satisfy $\frac{\mathrm{d}s_k(t)}{\mathrm{d}t}+\frac{\mathrm{d}\rho_k(t)}{\mathrm{d}t}+\frac{\mathrm{d}r_k(t)}{\mathrm{d}t}+\frac{\mathrm{d}q_k(t)}{\mathrm{d}t}=0$, in agreement with the normalization condition (7).

Since $\theta(t)$ at any time step t is much smaller than unity, by the same method as in Ref.[9], we can omit its higher order term in Eqs.(8) and (9), then the following set of coupled approximate equations can be obtained:

$$\frac{\mathrm{d}s_k(t)}{\mathrm{d}t}=-\lambda k s_k(t)\theta(t)-s_k(t)\theta(t), \tag{12}$$

$$\frac{\mathrm{d}\rho_k(t)}{\mathrm{d}t}=-\rho_k(t)+\lambda k s_k(t)\theta(t), \tag{13}$$

$$\frac{\mathrm{d}r_k(t)}{\mathrm{d}t}=\rho_k(t), \tag{14}$$

$$\frac{\mathrm{d}q_k(t)}{\mathrm{d}t}=s_k(t)\theta(t). \tag{15}$$

The initial conditions of Eqs.(12)–(15) are

$$s_k(0)\approx 1,\quad \rho_k(0)\approx 0,\quad r_k(0)=0,\quad q_k(0)=0. \tag{16}$$

It is difficult to solve the above equations analytically, but with the initial conditions (16) and the final epidemic condition$\rho_k(\infty)=0$, we can find out the epidemic spreading threshold of the QSIR model.

From Eqs.(12) and (16), we can obtain

$$s_k(t)=\mathrm{e}^{-(\lambda k+1)\int_0^t\theta(\tau)\mathrm{d}\tau}. \tag{17}$$

Define an auxiliary function

$$\phi(t)=\int_0^t\theta(\tau)\mathrm{d}\tau. \tag{18}$$

From Eq.(5), we have

$$\begin{aligned}\phi(t)=&\int_0^t\theta(\tau)\mathrm{d}\tau\\ =&\int_0^t\left[\frac{1}{\langle k\rangle}\sum\nolimits_k kp(k)\rho_k(\tau)\right]\mathrm{d}\tau\\ =&\frac{1}{\langle k\rangle}\sum\nolimits_k kp(k)\int_0^t\rho_k(\tau)\mathrm{d}\tau.\end{aligned}$$

Using Eqs.(14) and (16), we can further obtain $r_k(t)=\int_0^t\rho_k(\tau)\mathrm{d}\tau$, hence

$$\phi(t)=\frac{1}{\langle k\rangle}\sum\nolimits_k kp(k)r_k(t). \tag{19}$$

In order to gain a closed relation for the total density of infected individuals, let us compute the time derivative of $\phi(t)$:

$$\begin{aligned}\frac{\mathrm{d}\phi(t)}{\mathrm{d}t}=&\frac{1}{\langle k\rangle}\sum\nolimits_k kp(k)\rho_k(t)\\ =&\frac{1}{\langle k\rangle}\sum\nolimits_k kp(k)[1-s_k(t)-r_k(t)-q_k(t)]\\ =&1-\phi(t)-\frac{1}{\langle k\rangle}\sum\nolimits_k kp(k)\mathrm{e}^{-(\lambda k+1)\phi(t)}\\ &-\frac{1}{\langle k\rangle}\sum\nolimits_k kp(k)q_k(t).\end{aligned} \tag{20}$$

From Eqs.(15) and (16), we have

$$q_k(t)=\int_0^t s_k(\tau)\theta(\tau)\mathrm{d}\tau. \tag{21}$$

Since $s_k(\tau)$ is an un-increasing function of τ and non-negative, according to the mid-value theorem of integral, we have

$$q_k(t)=s_k(0)\int_0^c\theta(\tau)\mathrm{d}\tau\approx\int_0^c\theta(\tau)\mathrm{d}\tau=\phi(c) \tag{22}$$

where $0<c<t$. Since at the end of the epidemic process (or equally when $t\to\infty$), $\frac{\mathrm{d}\phi(t)}{\mathrm{d}t}=0$ and

$\rho_k(\infty) = 0$, combining Eq.(20) with Eq.(22) we can obtain

$$\phi(\infty) = 1 - \frac{1}{\langle k\rangle}\sum\nolimits_k kp(k)\mathrm{e}^{-(\lambda k+1)\phi(\infty)} - \phi(c), \tag{23}$$

where $0 < c < \infty$. From Eqs.(5) and (18) we know that

$$0 \le \phi(c) \le \phi(\infty). \tag{24}$$

Therefore, $\phi(\infty)= 0$ is always a solution of Eq.(13). In order to obtain a non-zero solution, we perform a Taylor expansion at $\phi(\infty)=0$ to the exponential function in Eq.(23):

$$\mathrm{e}^{-(\lambda k+1)\phi(\infty)} = 1 - (\lambda k+1)\phi(\infty) + \frac{1}{2}(\lambda k+1)^2\phi^2(\infty)\mathrm{e}^{-\xi}, \tag{25}$$

where $0 < \xi < (\lambda k + 1)\phi(\infty)$. Substitute this result in Eq.(23), we can further obtain

$$\phi(\infty) \le \left(\frac{\lambda < k^2 >}{\langle k\rangle} + 1\right)\phi(\infty) - \phi(c). \tag{26}$$

From Eq.(26), we have

$$\lambda \ge \frac{\langle k\rangle}{\langle k^2\rangle}\cdot\frac{\phi(c)}{\phi(\infty)}. \tag{27}$$

This condition defines the epidemic threshold

$$\lambda_{\mathrm{c}} = \frac{\langle k\rangle}{\langle k^2\rangle}\cdot\frac{\phi(c)}{\phi(\infty)}. \tag{28}$$

Compare Eq.(28) with Eq.(6), we can see that the QSIR model has a similar epidemic threshold to that in the SIR model, both of which are very small on the large uncorrelated complex networks.

4. Simulations for QSIR and SIR models

To compare the epidemic prevalence $r(\infty)$ of the QSIR model with that of the SIR model on the uncorrelated complex networks, we have applied the two models to several BA networks. We constructed the BA networks with the following algorithm: Starting from m_0 nodes that are connected with each other, at every time step a new node is added, with m ($m \le m_0$) edges that are connected to an old node i of the network with probability

$$\Pi(k_i) = \frac{k_i}{\sum_j k_j}, \tag{29}$$

where k_i is the degree of node i. After iterating this scheme $N - m_0$ times, a network with size N is built. The degree distribution of this network is (see Ref.[16]):

$$p(k) = \frac{2m(m+1)}{k(k+1)(k+2)}, \quad \text{for} \quad k \ge m \tag{30}$$

and the average degree $\langle k\rangle = 2m$.

We have built such BA networks with sizes N from 10000 to 20000 and m from 2 to 10. Initially, we randomly infected 50 nodes for each of the networks, so that the initial conditions satisfy Eq.(16) for the nodes with degree k. Also, to each of the above networks, we applied the QSIR and the SIR models at epidemic spreading rate λ=0.1, 0.2, 0.3 and 0.4 separately. All the results show that the epidemic prevalence $r(\infty)$ of the QSIR model is less than that of the SIR model with the same parameters N, m and λ. The following figures are only some of the typical ones of the simulations.

Figure 1 shows the epidemic processes of the SIR and the QSIR models on the BA network with N=20000 and m=2. Since the epidemic thresholds of the SIR and QSIR models are both approximately $\lambda_{\mathrm{c}} \approx \frac{\langle k\rangle}{\langle k^2\rangle} = \frac{\sum_{k=2}^{N} kp(k)}{\sum_{k=2}^{N} k^2p(k)}$. Averaged over 10 runs of the generated BA networks, $\lambda_{\mathrm{c}} \approx 0.0600$ is obtained. Hence we should choose $\lambda > 0.0600$ in order to make sure that the disease can spread on the network. All the simulations in Fig.1 are averaged over 10 runs of epidemic spreading process.

Figure 2 shows the epidemic prevalence predicted by the SIR and the QSIR models on the BA network with N=20000 and m=5. The epidemic thresholds of the two models on this network are both $\lambda_{\mathrm{c}} \approx 0.0328$ (averaged over 10 runs of the generated BA networks). This figure shows that: for any fixed epidemic spreading rate λ, the epidemic prevalence $r(\infty)$ shown by the QSIR model is less than that by the SIR model.

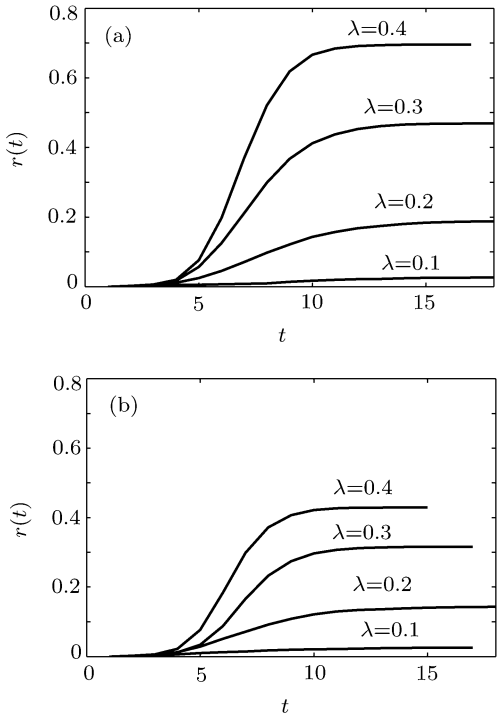


Fig.1. Comparison of epidemic prevalence on the BA network with N=20000 and m=2: (a) SIR model, (b) QSIR model.

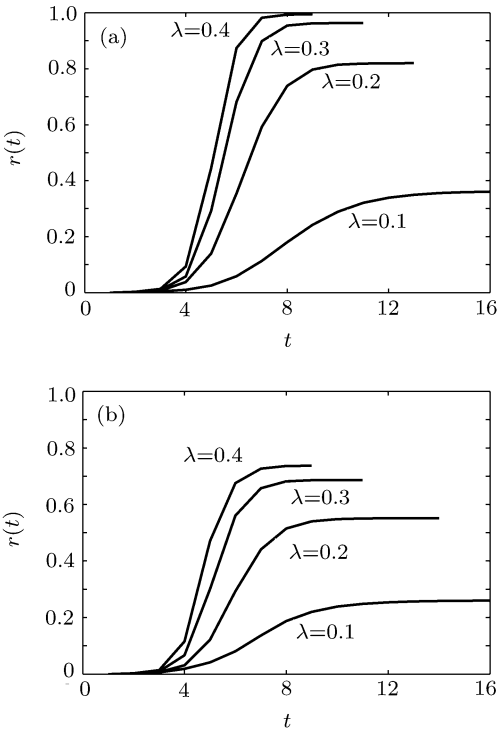


Fig.2. Comparison of epidemic prevalence on the BA network with N=20000 and m=5: (a) SIR model, (b) QSIR model.

From Figs.1 and 2 we can find that the parameter m also affects the epidemic prevalence shown by the two models. For a fixed spreading rate λ, the larger the m is, the higher the epidemic prevalence of the two models is. This shows that it is easier for a disease to spread on a more connected network. Figure 3 shows this information clearly.

In Fig.3, the BA networks have a size N=20000 with m=2 to 10, the epidemic spreading rate λ=0.2 (each simulation value is the average over 10 runs). From the figure we can see that the epidemic prevalence $r(\infty)$ of the two models are both the increasing functions of m. Figure 3 also shows the following fact: for a fixed spreading rate λ ($\lambda > \lambda_c$), as the connecting parameter m is getting larger, the epidemic prevalence $r(\infty)$ by the SIR model will tend to 1, and by the QSIR model will tend to a fixed value (< 1). For example, in this figure when m=10, $r(\infty) \approx 0.9906$ for the SIR model, and $r(\infty) \approx 0.7543$ for the QSIR model. In other words, for a fixed spreading rate λ, when m is large enough, the SIR model always predicts that about 100% of the individuals will be infected by the disease!

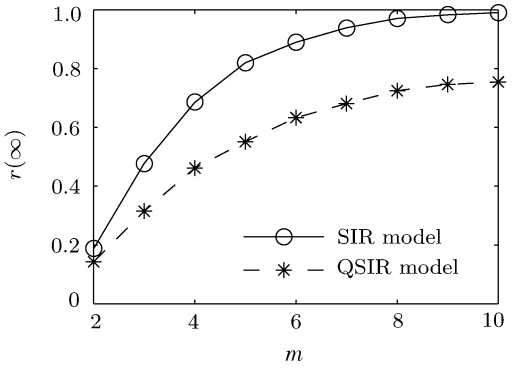


Fig.3. Relations between the epidemic prevalence $r(\infty)$ and the parameter m for λ=0.2.

Figures 1 and 2 also show the fact: when m is fixed, the larger the λ is, the higher the epidemic prevalence of the two models is. This result can be seen in Fig.4.

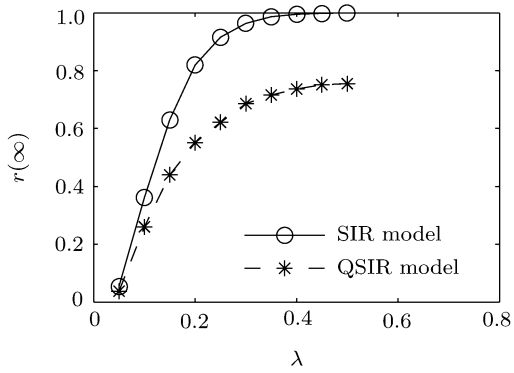


Fig.4. The epidemic prevalence $r(\infty)$ versus the spreading rate λ at m=5.

Figure 4 shows another fact: at a fixed connecting parameter m, as the spreading rate λ is getting larger, the epidemic prevalence $r(\infty)$ by the SIR model will tend to 1, and that by the QSIR model will tend to a fixed value. For example, in this figure when λ=0.5, $r(\infty) \approx 0.9993$ for the SIR model, and $r(\infty) \approx 0.7553$ for the QSIR model. In other words, for a fixed connecting parameter m, when spreading rate λ is large enough, the SIR model always predicts that about 100% of the individuals will be infected by the disease!

Figure 5 gives more detailed information of the epidemic processes described by the SIR and the QSIR model. In this figure, the BA network is of a size N=20000 and m=5. The epidemic threshold is $\lambda_c \approx 0.0328$ and the spreading rates are λ=0.1, 0.2, 0.3 and 0.4. The figure shows how the densities of the three state nodes ($\rho(t)$ for the infected, $r(t)$ for the recovered and $q(t)$ for the quarantined) are changing as time changes.

It should be noted that for the QSIR model, the density of the recovered nodes increases as the spreading rate λ increases, but the density of the quarantined nodes does not always follow the same rule. This is in agreement with the fact that the sum of $r(\infty)$ and $q(\infty)$ is always less than or equal to 1.

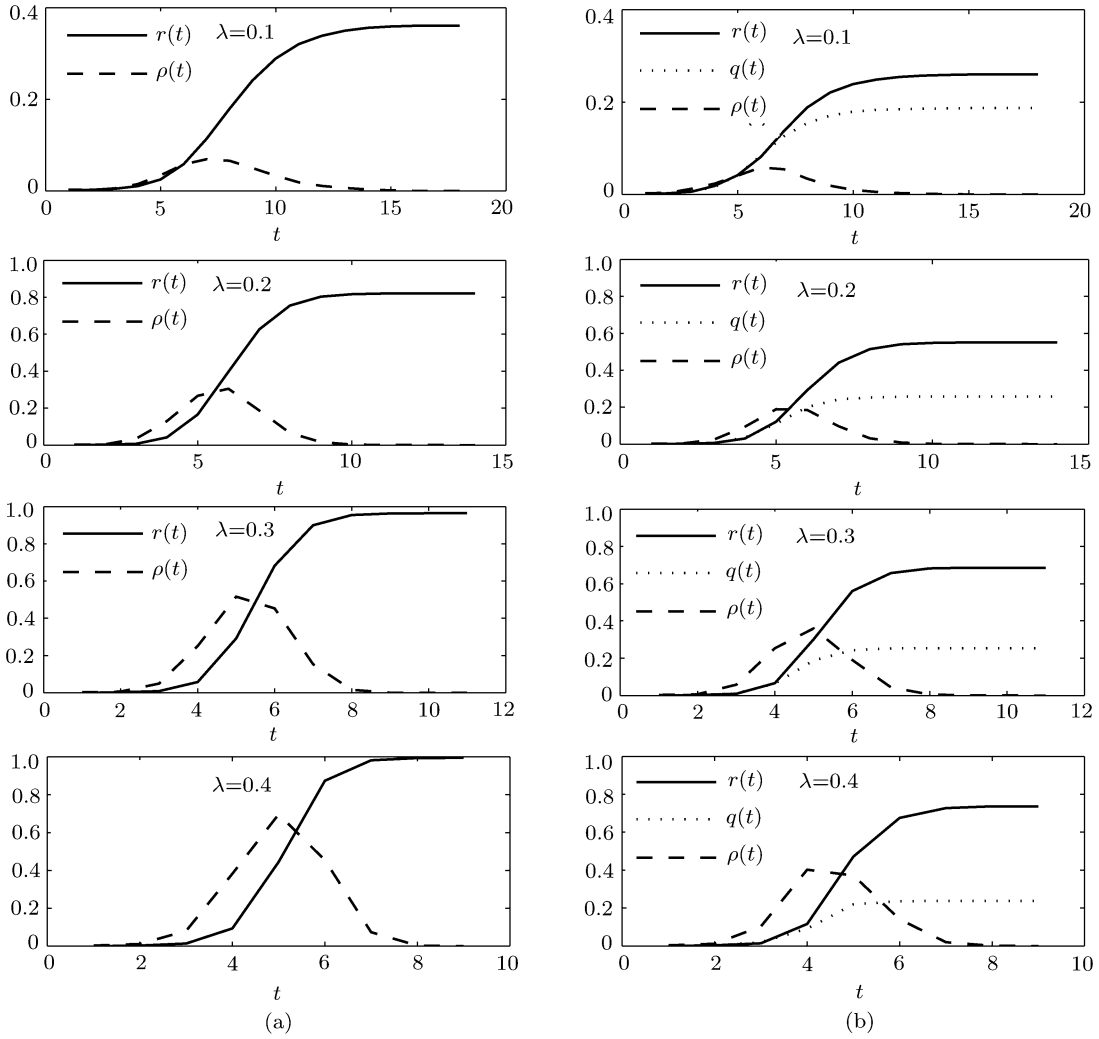


Fig.5. Epidemic processes on the BA network with N=20000 and m=5: (a) SIR model, (b) QSIR model.

5. Conclusions

In this paper, we have proposed a dynamic epidemic control model, QSIR model, on the uncorrelated complex networks. Based on the classical SIR model, we added a dynamic quarantining state to control the epidemic spreading. At any time, a sus-

ceptible node may become quarantined depending on the probability that any edge points to an infected node. By means of theoretical analysis, we find that the QSIR model has the same epidemic threshold as the SIR model does on the uncorrelated complex networks, but it shows that the prevalence of the infected individuals can be reduced remarkably compared with that of the SIR model. We hope our work may be helpful in understanding the epidemic spreading phenomena on real networks and designing appropriate strategies to control infections.

References

[1] Xu D, Li X and Wang X F 2007 *Acta Phys. Sin.* **56** 1313 (in Chinese)

[2] Li Y, Liu Y, Shan X M, Ren Y, Jiao J and Qiu B 2005 *Chin. Phys.* **14** 2153

[3] Hu K and Tang Y 2006 *Chin. Phys.* **15** 2782

[4] Barthelemy M, Barrat A, Pastor-Satorras R *et al* 2004 *Phys. Rev. Lett.* **92** 178701

[5] Moore D, Shannon C, Voelker G M and Savage S 2003 in: *Proceedings of the IEEE Inforcom*, 1901-1910, San. Francisco, CA

[6] Williamson M M 2002 in: *Proceedings of ACSAC Security Conference*, 61–68, Las Vegas

[7] May R M and Lloyd A L 2002 *Phys. Rev.* E **64** 066112

[8] Barthelemy M, Barrat A, Pastor-Satorras R and Vespignani A 2005 *Journal of Theoretical Biology* **235** 275

[9] Moreno Y, Pastor-Satorras R and Vespignani A 2002 *Eur. Phys. J.* B **26** 521

[10] Newman M E J 2003 *SIAM Review* **45** 167

[11] Wong C, Wang C, Song D, Bielski S and Ganger G R 2004 in: *Proceedings of the International Conference on Dependable Systems and Networks* (DSN-2004), 62–71, Florence, Italy

[12] Boguñá M and Pastor-Satorras R 2002 *Phys. Rev.* E. **66** 047104

[13] Zou C C, Gao L, Gong W and Towsley D 2003 in: *Proceedings of the 10th ACM International Conference on Computer and Communications Security* (CCS) 190–199, ACM Press

[14] Watts D J and Strogatz S H 1998 *Nature* **393** 440

[15] Liu Z R, Yan J R, Zhang J G and Wang L 2006 *Chin. Phys. Lett.* **23** 1343

[16] Albert R and Barabási A-L 2002 *Reviews of Modern Physics* **74** 47-97

[17] Wong W G, Ni S J, Shen S F and Yuan H Y 2007 *Acta Phys. Sin.* **56** 1938 (in Chinese)

[18] Yan D and Qi G N 2006 *Acta Phys. Sin.* **55** 3799 (in Chinese)

[19] Chen F, Chen Z Q and Yuan Z Z 2007 *Chin. Phys.* **6** 287